Heritage Science

RESEARCH

Open Access

Analysis of the stakes of the Xianyang Ancient Ferry Site, Shaanxi, China

Gele Teri[1], Peng Fu[2], Kezhu Han[1], Dan Huang[1], Yanli Li[1], Yujia Luo[1*], Huiping Xing[1*] and Yuhu Li[1*]

Abstract

Historical records indicate that Xianyang Ancient Ferry Site, dating back over three millennia to the late Shang Dynasty, has been an important transportation hub in ancient times. The use of combined wooden stakes and stones is a special method for flood control among ancient flood prevention techniques. This research aims to evaluate the current preservation condition of these ancient wooden stakes. The dating of the wooden stakes at the site ranges between 940 ± 30 BP and 320 ± 30 BP. The fiber cross-section and microstructure images of the wooden samples indicate that the wood is attributed to *Platycladus orientalis*. SEM images indicate decay and deterioration of the wooden samples, with the presence of mold spores within the cavities. XRD, FTIR, and TG/DSC spectra of historical wooden samples collected from the site and fresh *Platycladus orientalis* wood samples demonstrate a significant decrease of cellulose crystallinity in the historical samples, leading to severe deterioration of the wood at the site. Five dominant mold species were identified, i.e., *Aspergillus niger, Aspergillus flavus, Penicillium citrinum, Trichoderma,* and *Phanerochaete chrysosporium*, which accelerate the degradation of cellulose and other polysaccharides. This research provides scientific evidence for the selection of reinforcement materials and guides curators and conservators to formulate conservation strategies in the future.

Keywords The Xianyang Ancient Ferry Site, Wood characterization, Microbiological analysis, *Platycladus orientalis*

Introduction

The Xianyang Ancient Ferry Site, located adjacent to Xianyang Lake in Xianyang City, Shaanxi Province in China (Fig. 1A, B), was discovered in 2002 by Xianyang archaeologists when cleaning a river channel. This discovery unveiled a segment of an old river dike, marking the location of the Xianyang Ancient Ferry Site [1, 2]. The unearthing of the site holds immense significance for the study of ancient transportation, commerce, military strategy, literature, and urban evolution, garnering widespread attention from various societal sectors. The Xianyang Ancient Ferry Site Museum (Fig. 1C), established on the foundation of the Ming and Qing dynasty ferry site (1371AD ~ 1908 AD), was officially designated as a cultural heritage conservation unit of the Shaanxi province on October 9, 2008 [2].

The Xianyang Ancient Ferry, situated at the Wei River crossing in Xianyang, traverses the central part of Shaanxi Province. Historically, individuals traveling north and south near Xianyang and Chang'an consistently utilized this ferry crossing to traverse the Wei River. Due to the river's seasonal fluctuations in water level, both pontoon bridges and boats have been traditionally employed; in the winter and spring, pontoon bridges are predominantly used, in the summer and autumn, people tend to use ferry boats [3]. Historically, the Xianyang Ancient Ferry has evolved from the Qin Dynasty (211

*Correspondence:
Yujia Luo
yujialuo@snnu.edu.cn
Huiping Xing
xhp@snnu.edu.cn
Yuhu Li
liyuhu@snnu.edu.cn
[1] Engineering Research Center of Historical Cultural Heritage Conservation, Ministry of Education, School of Materials Science and Engineering, Shaanxi Normal University, Xi'an 710119, China
[2] Shaanxi Institute for the Preservation of Culture Heritage, Xi'an 710075, China

Fig. 1 **A**, **B** The location map of the Xianyang Ancient Ferry Site; **C** The Xianyang Ancient Ferry Site Museum; **D** The display area of the wooden pile in the museum; **E** The wooden piles of the site

BC) to the Qing Dynasties (1912 AD), transforming over more than 3000 years, during which it also served as a strategic point on the ancient Silk Road. Excavations at the site have unearthed plenty of artifacts, such as coins, ceramics, jades, iron rings used for mooring boats, and remnants of river embankments from the Ming and Qing Dynasties (1368–1912 AD). These artifacts provide important material evidence for studying the economic, cultural, and military aspects of the period. Also, several Buddhist statues found at this site demonstrate the Buddhist cultural exchanges with the Western Regions[4].

At the Xianyang Ancient Ferry Site, the discovered wooden piles serve as a foundation to control floods (Fig. 1D, E), which were found to be buried beneath the stones, serving as a foundation (Fig. 2). These wooden piles, inclined southward in alignment with the tilt of the stones, were spaced 6–26 cm apart and had diameters ranging from 10 to 20 cm. These wooden piles are considered as precious heritage objects, significantly contributing to the in-depth study and enrichment of the historical development of China's flood control and hydraulic engineering. The projects for controlling floods mark a vital phase in human civilization, with the interaction between humans and rivers playing an essential role in pre-modern societies. Under proper management, rivers can serve as an important source of water supply, navigation, and agricultural irrigation; on the contrary, floods can be induced under poor management, where historical records have shown that floods are one of the most destructive natural disasters [5].

Humans have accumulated an increasing wealth of knowledge in river management and flood control for thousands of years, with the construction of embankments being an effective measure [6, 7]. In the past, stone embankments were commonly built to control floods, e.g., a 12-km-long stone embankment was constructed along the upper and lower reaches of the Yongding River to withstand floods from the Yuan to the Qing dynasty (1271–1912AD) [8]. Fascines were employed as protective structures against floodwaters and to reinforce embankments, made from reeds, bamboo, willow branches, mud, and gravel, which were bound into cylindrical shapes, with subsequent layers pressed onto the outer surface of the first, forming a structural barrier [9, 10]. These structures mitigated damages caused by the rushing water, protecting riverbanks by reducing slope steepness and establishing physical barriers against surface runoff. In 1730, Forest de Bélidor also recommended fascines as an alternative stone paving to mitigate damages at the bottom of water gates [10]. Similarly, fascines were widely used in ancient Chinese water projects, applied to numerous rivers such as the Yangtze, Yellow, and Huai Rivers, as well as in sea dyke and dock projects [11, 12]. Particularly in the flood control management of the Yellow River basin, fascines played a crucial role in embankment reinforcement and breach closure [13].

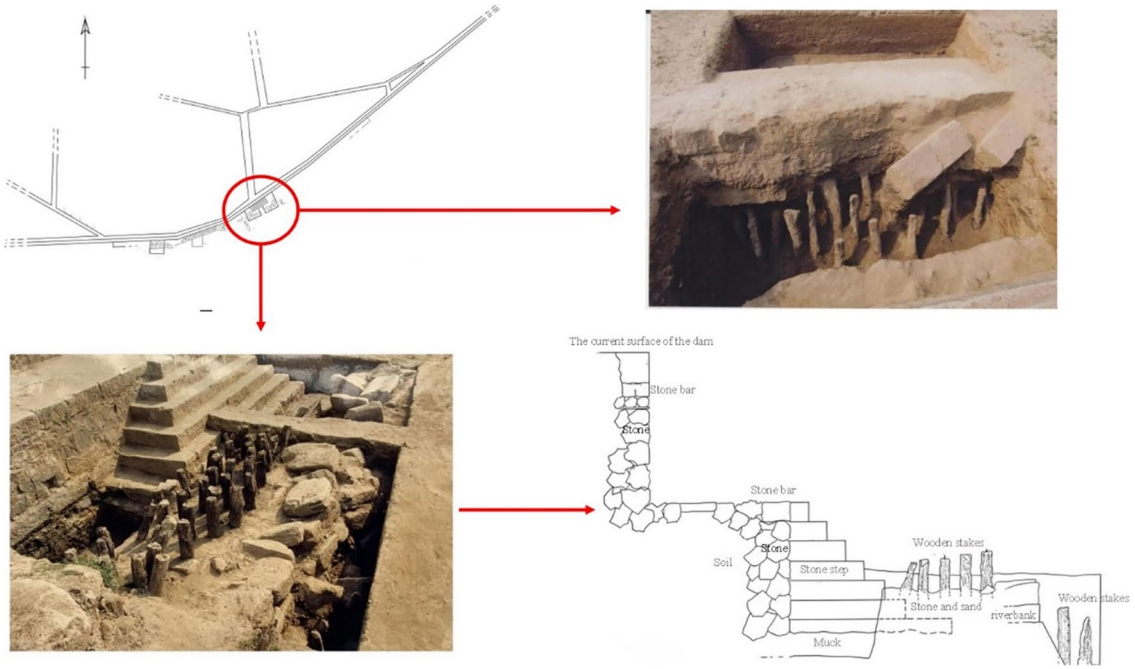

Fig. 2 Diagram of the excavation site of the Ming and Qing Dynasty River dikes at the Xianyang Ancient Ferry Site

Overall, the combination of wooden stakes with stone blocks effectively addressed the issue of stone dikes built on riverbanks being frequently washed away due to the lack of a solid foundation. This technological advancement represented a bold innovation in the history of dike construction at the time, reflecting the ingenuity and wisdom of our ancestors. As recorded in historical documents named Xiangyang Zhi, this method has allowed the Qing Dynasty (1745 AD) stone dike to be preserved for nearly 200 years, which remains intact at over 70 m. This evolution demonstrates a historical transition in engineering quality from rudimentary to sophisticated, and from lenient to stringent standards, indicating a significant enhancement in technical expertise. Also, this example provides valuable insights for contemporary river dike construction in terms of technical and quality management. The analysis of the wooden piles collected from the site could enrich our knowledge of ancient technology of flood control. Currently, this collection of wooden artifacts is housed in the exhibition hall of the Xianyang Ancient Ferry Site Museum. No further restoration treatments were performed since the wooden objects were excavated in 2002. Also, due to the lack of management of environmental temperature and relative humidity, the wooden objects are in poor condition.

Understanding the detailed chemical structure, cellulose crystal structure, and cell wall porosity of waterlogged wooden artifacts is essential for their protection and reinforcement. Such studies provide essential data support and guide for dehydration and strengthening treatments. The 196th meeting of the American Chemical Society in 1988, themed "Archaeological Wood: Properties, Chemistry, and Preservation," marked the first systematic and comprehensive summary of the structure and performance of archaeological wood [14]. Subsequently, the use of a series of techniques, such as field emission transmission electron microscopy, two-dimensional solid-state nuclear magnetic resonance, Raman imaging technology, dynamic vapor sorption analysis [15], and dynamic mechanical analysis [16], has been reported. In particular, theoretical research in areas such as anatomical structure [17], cell wall components and chemical structures [18, 19], cellulose crystal structures [20, 21], porosity structures [22], and mechanical properties [23] has been gradually studied. A variety of spectroscopic analysis techniques—including Fourier-transform infrared spectroscopy (FTIR), near-infrared spectroscopy (NIR), Raman spectroscopy, and nuclear magnetic resonance (NMR)—along with thermochemical methods such as thermogravimetric analysis (TGA), pyrolysis mass spectrometry (Py-MS), and pyrolysis gas chromatography-mass spectrometry (Py-GC/MS), have been increasingly applied to the study of chemical structure changes in archaeological wood [15, 24–28]. The maturation of infrared imaging and Raman imaging technologies has enabled more effective analysis of the

chemical structure of archaeological wood [15, 29], making these techniques viable alternatives for studying the chemical structures of wood cell walls. Currently, crystal structure research employs techniques such as X-ray diffraction (XRD) and wide/small-angle X-ray scattering (WAXS/SAXS). XRD, an accessible and straightforward method using wood powder, can determine information such as cellulose crystal peak types, relative crystallinity, and crystal sizes [30, 31].

In this study, we aim to identify and analyze the wood species used in the piles and assess their degree of deterioration, in order to guide future conservation treatments. Given the variety of wood materials used in the past and the aging conditions of wooden materials [32], identification of the species of ancient wooden materials can be challenging [33]. Microscopic observation of wood morphological characteristics using stereomicroscopes, optical microscopes, and electron microscopes is a critical part of the identification and classification process [34–39]. The application of light and scanning electron microscopy (SEM) in heritage research is commonly used, particularly in the study of degraded wooden structures in archaeological wood, as it provides characteristic information related to the deterioration conditions of wooden materials [37, 40–43]. In order to keep the wooden objects intact as much as possible, techniques requiring small amount of samples were used, such as the determination of the crystallinity of cellulose using X-ray diffraction (XRD), an important indicator of wood degradation, and the use of Fourier transform infrared microscopy (FTIR) to study the changes in wood chemical compounds.

We therefore selected a small test area from the Xianyang Ancient Ferry Site to assess the preservation condition of the piles. In addition, radiocarbon dating (^{14}C), fiber observation, thermogravimetric analysis (TGA), and scanning electron microscopy (SEM) coupled with energy-dispersive X-ray spectroscopy, were also used to assess the wood sample of the Xianyang Ancient Ferry Site. Additionally, we isolated and identified the dominant microbial communities on the wood surface. This research provides important scientific information on the ancient wooden piles prior selection of flood control techniques used during the Ming and Qing dynasties in China.

Materials and methods

Samples of wooden stakes

Considering a large number of wooden piles, samples were taken from four piles within a limited test area (Fig. 3C), in compliance with the requirements of the Cultural Heritage Conservation Department of the Xianyang Ancient Ferry Site. Samples were collected from the cracked and detached parts of the piles. The sizes of the samples varied, with the largest being approximately 5 cm × 1 cm × 1 cm, to assess the degree of deterioration of the wooden material.

Radiocarbon dating

According to the conditions of the test center, four 15 mg wooden samples were weighed and used for dating testing. The radiocarbon dating in this study was conducted at Beta Analytic Radiocarbon Dating Laboratory (Miami, USA), employing four internal NEC Accelerator Mass Spectrometers and four Thermo Isotope Ratio Mass Spectrometers (IRMS). The conventional radiocarbon ages were calculated using the Libby half-life (5568 years), corrected for isotopic fractionation, and rounded to the nearest decade. Results are reported as radiocarbon years before present (BP), with "present" defined as AD 1950. Sample pretreatment and radiocarbon dating followed the method described in the study of Francisco Martínez-Sevilla et al. [44].

Sample morphology preparation

Only one of the four samples adheres to specifications of sample size for cross-sectional morphology observation. Therefore, 1 cm × 1 cm × 1 cm wooden sample was embedded in epoxy resin. Cross-sections of the dried resin were prepared using an ultramicrotome (EM UC7, Leica, Germany). The resins were then mounted on slides and the microstructure of the samples was observed using an optical microscope (XWYVI, Zhuhai Walron Paper Technology Co., Ltd., China).

SEM and EDX analysis

The same sample used for the observation of wood cross-sections was used for microscopic observation for subsequent data comparison. The samples were cut into thin slices (1–2 μm) and pasted to the sample stage using the conductive adhesive. Subsequently, the surface of the samples was sprayed with gold to enhance conductivity. The microstructure was observed and energy spectrum analysis of the samples was conducted using a scanning electron microscope coupled with energy-dispersive X-ray spectroscopy (SEM–EDX, SU3500, Hitachi, Japan). Acceleration voltage is set to 10 kv, beam spot strength is 30, working distance is 8.8 mm.

X-ray diffraction analysis

The crystallinity of the wooden samples collected from the site was compared with that of fresh *Platycladus orientalis* wood samples (inside of the wood) using a high-resolution X-ray diffractometer (XRD, Smart Lab 9, Rigaku Corporation, Japan), where 1 g of sample powder was used. The test conditions were set for Cu Kα

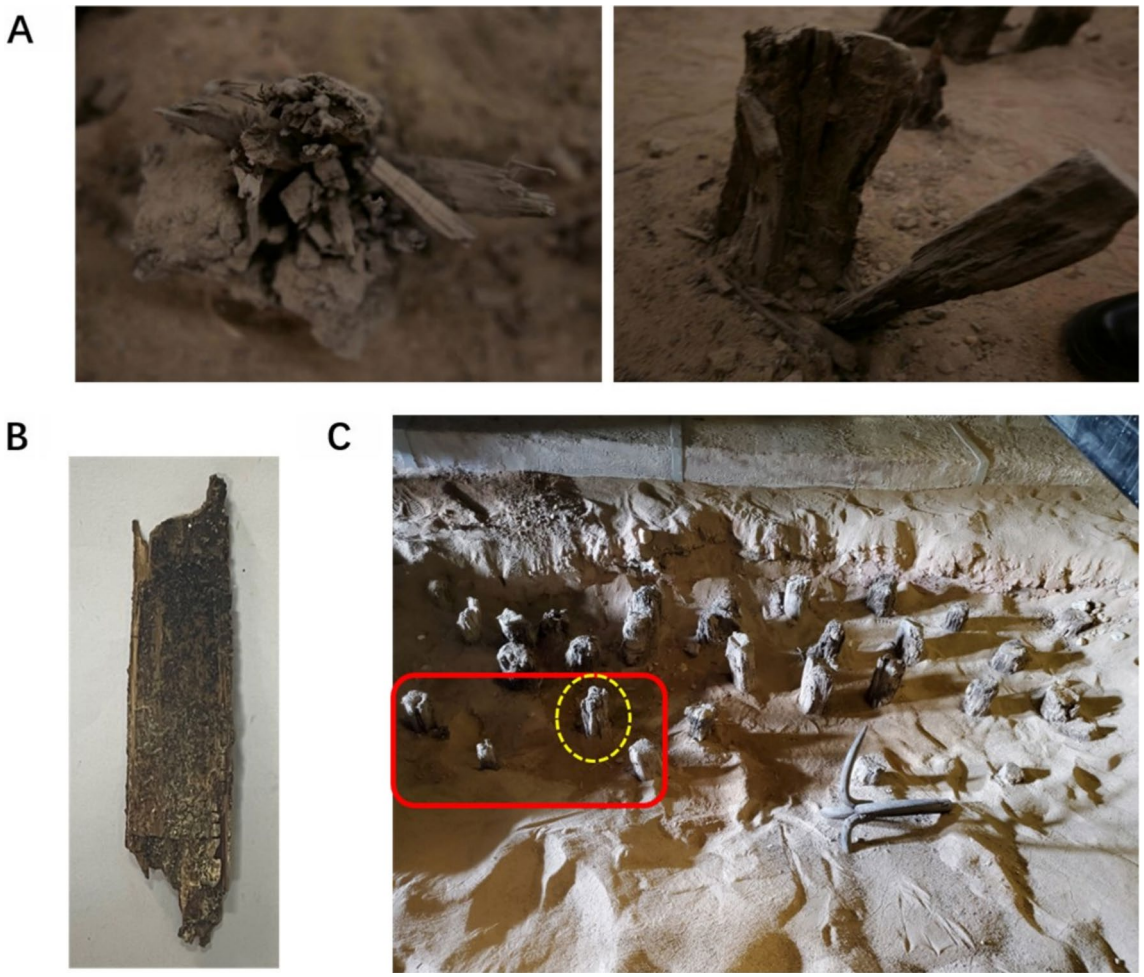

Fig. 3 **A** Current preservation condition of the Xianyang Ancient Ferry Site; **B** The wood sample; **C** the Xianyang Ancient Ferry Site test area (the yellow circle is typical)

radiation (λ = 1.54056 Å), with a 2θ range of 20°–80°, an acceleration voltage of 45 kV, a tube current of 200 mA, and a scanning speed of 5°/min. All four wooden pile samples were used for XRD analysis, where three spectra were collected for each sample and the average was used. Given that all samples present similar data patterns, the XRD spectrum of the sample with a greater degree of degradation was presented in this study.

As supported by the crystallinity index calculated using the Segal method [45]:

$$CrI = \frac{I_{002} - I_{am}}{I_{002}} \times 100$$

In the above equation, CrI is the relative crystallinity index, I_{002} is the maximum intensity of the diffraction surface, and I_{am} represents the intensity of the non-crystalline background diffraction when the 2θ angle is close to 18°.

Infrared absorption spectroscopy

2 mg of powder of the wooden samples collected from the site and fresh *Platycladus orientalis* wood samples were used to prepare KBr pellets, which were then used to collect FTIR spectra using the Fourier transform infrared spectrometer (Nicolet iS10, Thermo Fisher Scientific, USA). The spectral range was set between 4000 and 400 cm^{-1}, with the resolution of 4 cm^{-1}, and both sample and background were scanned 64 times. The molecular structures of the samples were identified through the characteristic peaks of various functional groups in the spectra. All four wooden pile samples were used for FTIR analysis, where three spectra were collected for each sample and the average was used. Due to that all samples present similar data patterns, the FTIR spectrum of the sample with a higher degree of degradation was presented in this study.

Thermogravimetric analysis

15 mg sample from the site and fresh *Platycladus orientalis* wood samples were used for thermogravimetric analysis (Themys One, Setaram, France) to obtain the thermogravimetric curve of the wooden samples collected from the site, in order to assess its preservation state. During the test, nitrogen was used as the protective gas. The temperature range was set from 30 to 800 °C, with a heating rate at 10 °C/min. All four wooden pile samples were used for the thermogravimetric analysis, where three spectra were collected for each sample and the average was used. The thermogravimetric spectrum of the sample with a higher degree of degradation was presented in this study.

Microbial culturing of wooden samples and identification

The dominant microbial species in the wood of the Xianyang Ancient Ferry Site can be identified by analyzing the microorganisms in the test area. Immerse a cotton swab in a modest quantity of mold present on the wooden surface, promptly transfer the swab into a centrifuge tube containing normal saline, seal the tube with a film, and label it. All aforementioned instruments are sterilized prior to utilization. Samples collected from the site were cultured on Potato Dextrose Agar (PDA) medium for 48 h (Ouwo Biotechnology Co., Ltd.), and after microbial growth, individual colonies were isolated using an inoculation loop and transferred to PDA plates. This step was repeated until the culture dish contained only one type of microorganism. All the above procedures were conducted in a laminar flow cabinet. The purified microorganisms were sent to Shanghai Pasno Biotechnology Co., Ltd. (Shanghai, China) for species identification. 5 × 5 mm section was excised from a purified target bacterial colony and carefully extracted. This section was then cut into slices (thickness in 2 mm) on a glass slide and immersed in a 2.5% (v/v) glutaraldehyde solution. The samples were subsequently fixed overnight at 4 °C in a refrigerator for 12 h. After fixation, the samples were removed using tweezers and rinsed with sterile water every 30 min, with the process repeated three times. Dehydration of the rinsed samples was carried out using ethanol solutions of 30%, 50%, 70%, and 95% concentration, with each gradient treatment for 20 min. Following these dehydration steps, the samples were further dehydrated with anhydrous ethanol for 30 min. The completely dehydrated samples were then placed in an ultra-low temperature freezer at −80 °C overnight, removed, and dried using a vacuum freeze dryer. Gold sputtering was performed using an ion sputter (120 s, 20 mA) before the structural and morphological changes of the bacterial strains were observed using a scanning electron microscope (SU3500, Hitachi company, Japan).

Results and discussion

Structure of the wooden stakes-stones structure for flood control

The radiocarbon dating results yielded ages of approximately 1028–1172 AD, 1296–1400 AD, 1423–1500 AD, and 1540–1634 AD. It is worth noting that these ^{14}C dating results represent the growth age of the samples, rather than the construction age (Table 1). The discrepancy observed between the radiocarbon dates of the first sample and the remaining three samples may be attributed to one primary factors. The wooden stakes have been immersed in water for a long time, and the radiocarbon dating of objects originating from aquatic environments inevitably reflects the effect of this setting. The SEM–EDX analysis results (Figs. 5, 6) show that calcium-related compounds have also penetrated the intercellular spaces and cavities of the wood cells. Secondly, the effect of contaminants on the dating of wood or charcoal depends on the nature and degree of contamination and the age difference between the sample and the contaminants. If

Table 1 ^{14}C dating results of the wooden samples collected from the Xianyang Ancient Ferry Site

No	Laboratory number	14C dating	Calibration age	
			1σ (68.2%)	2σ (95.4%)
1	Beta—680,201	940 ± 30 BP	1113–1156 AD (32.3%) 1075–1107 AD (24.2%) 1040–1052 AD (8.7%) 1064–1068 AD (3%)	1028–1172 AD (95.4%)
2	Beta—680,196	620 ± 30 BP	1302–1328 AD (29.3%) 1348–1368 AD (21.1%) 1378–1395 AD (17.8%)	1296–1400 AD (95.4%)
3	Beta—680,200	430 ± 30 BP	1436–1473 AD (68.2%)	1423–1500 AD (91.4%) 1600–1616 AD (4%)
4	Beta—680,197	360 ± 30 BP	1472–1522 AD (35.7%) 1577–1624 AD (32.5%)	1540–1634 AD (49.9%) 1456–1529 AD (45.4%)

limestone is not adequately removed before AMS dating, the results may appear much older than the actual age of the wood or charcoal due to the geological origin of the limestone. Humic and fulvic acids, which adhere to the surfaces of wood and charcoal, can engage in carbon exchange during adsorption. This interaction can cause deviations in the dating results, making the samples appear either older or younger depending on the age of the organisms producing these organic acids. Additionally, the intrusion of roots can introduce modern carbon into the sample. Generally, ancient contaminants of unknown age tend to make the wood or charcoal samples appear significantly older, whereas modern carbon can make the samples appear much younger.

Microscope slice observations and SEM–EDX analysis

The current preservation condition of the wooden piles from the Xianyang Ancient Ferry Site is largely affected by severe biological deterioration. Figure 4 shows the microscopic structure of the wooden piles from the Xianyang Ancient Ferry Site on thecross section (A), radial section (B),tangential section (C). The wooden artifact samples exhibit the following anatomical characteristics: absence of vessels; coniferous wood; visible, relatively wide growth rings with a gradual transition from earlywood to latewood. In earlywood, tracheid cross-sections are square and polygonal with a single row of bordered pits on the radial walls, which are round or oval, and the pit apertures are circular. In latewood, tracheid cross-sections are rectangular, elliptical, and polygonal with a single row of circular bordered pits on the radial walls; the final rows of tracheids have notably thicker walls. The amount of axial parenchyma is minimal, dispersed in a stellate pattern. Wood rays are uniseriate, ranging from 1 to over 20 cells in height, typically between 3 and 12 cells; ray cells are exclusively composed of ray parenchyma cells, which are elliptical and often contain resin. No ray tracheids are observed; ray cell horizontal walls are thick, typically without pits, and end walls are often not septate and lack thickening. The cross-field pitting pattern between ray parenchyma cells and earlywood axial tracheids is of the Cupressus type, usually with 2 to 3 pits. Therefore, the wood sample has been identified as *Platycladus orientalis* from the family Cupressaceae, genus *Platycladus* [46, 47]. *Platycladus orientalis* is known for its strong resistance to decay and good durability, which is in line with historical records of its use at the ancient ferry site.

The surface of the wood samples is dark yellowish brown, with some parts being charcoal black, and containing small amounts of gravel (Fig. 3B). The wooden samples are quite brittle and have lost mechanical properties, demonstrating significant degradation of the wooden stakes. As shown in Fig. 5, SEM images of the wood samples reveal microbial decay and biological deterioration. Based on the findings in the literature, the presence of the phenomenon depicted in Fig. 5 suggests that the wood has undergone biodegradation [48]. The cross-sections of the wood show severe blockage in the cell lumen, The observation was made that mold (Fig. 5B, D) used with the wall of the cell cavity(Fig. 5A, C), with the presence of mold spores and gravel observable within these lumen (Fig. 5B, D). The tracheid cell walls exhibit a distinct small lumen (arrow 2 area in Fig. 5D), where weakened cells appear distorted, and some have collapsed. This indicates that the wood at the

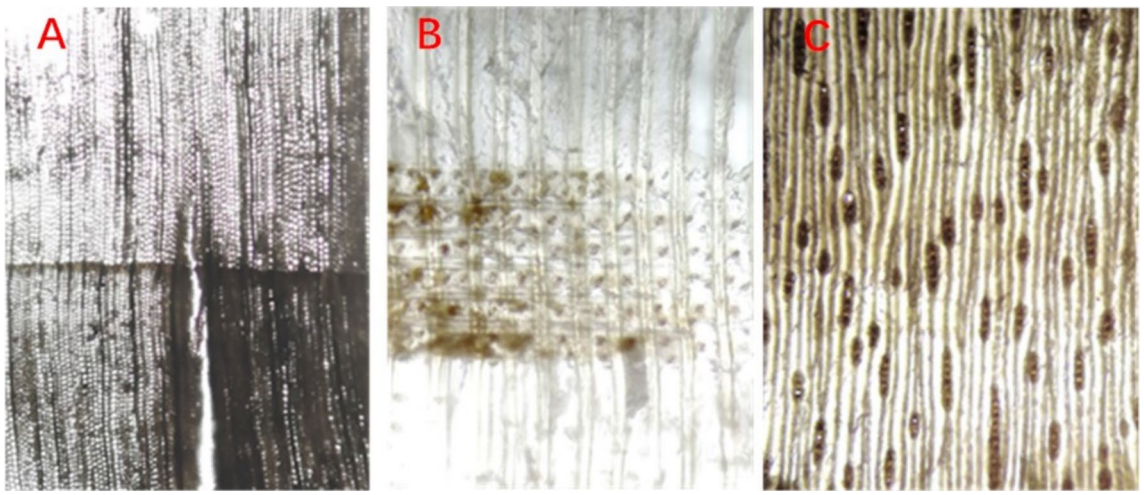

Fig. 4 Microstructure of the longitudinal section of the historical wooden samples collected from the Xianyang Ancient Ferry Site (**A** cross section, **B** radial section, **C** tangential section)

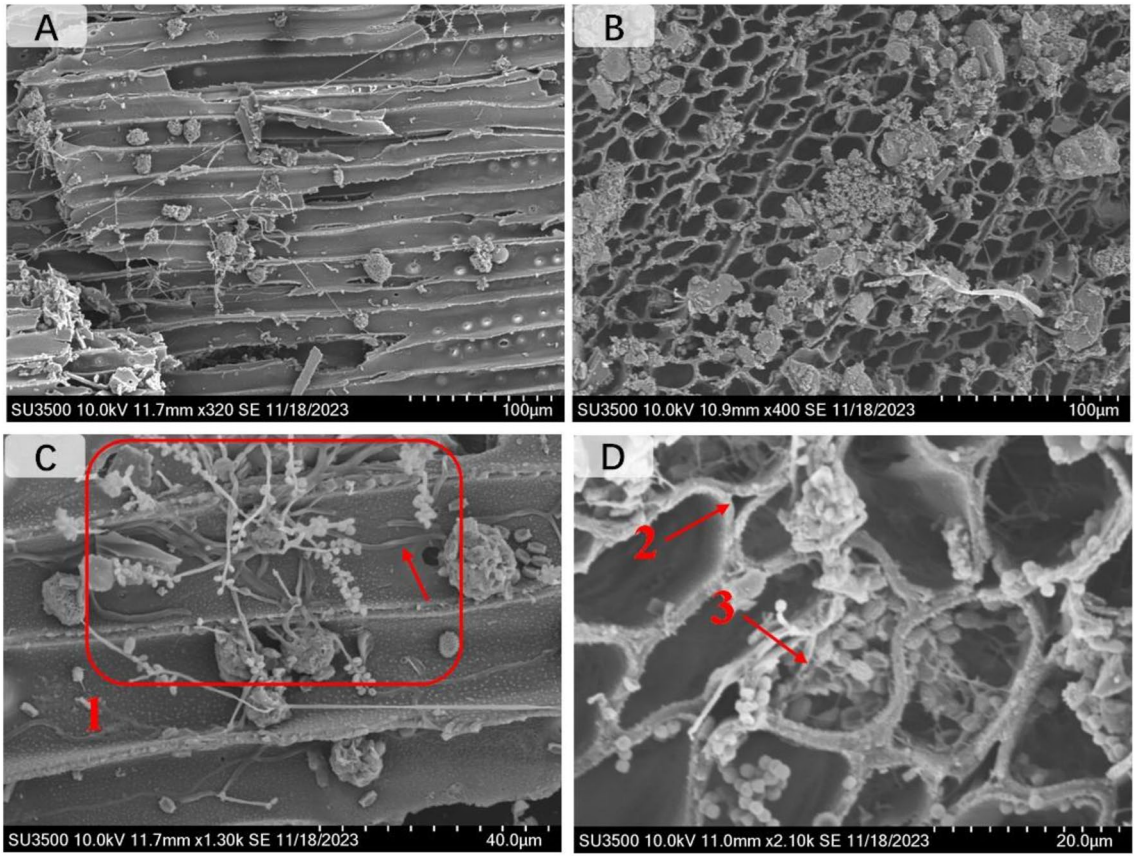

Fig. 5 SEM images of the historical wooden samples collected from the Xianyang Ancient Ferry Site. **C**, **D** illustrate a local enlargement of (**A**, **B**), respectively; **C**: Fungal hyphens (arrows) along the tracheids wall.1: Fungal hypha; 2: Cell wall atrophy and deformation; 3: Fungal spores in a cell cavity)

site has undergone significant decay, where microbial corrosion accelerates the degradation process in a humid environment.

Figure 6 presents the mapping image of the historical wooden samples, predominantly composed of carbon (C) and oxygen (O), with their respective concentrations being 21% and 22%. Additionally, other detected elements such as Na, Mg, Al, Si, S, and Ca can be attributed to the wood material and the long-term burial environment, during which elements from the surrounding soil, specifically Ca, Na, Mg, Al, Si, and S, penetrated the interstitial spaces and cavities of the wood cells. The inorganic content in wood is less than 1%. It comprises various proportions of silicon, aluminum, iron, calcium, magnesium, sodium, potassium, titanium, manganese, and heavy metals. Zając et al. [49] classified these into three categories, i.e., macronutrients including Ca, K, P, and S; micronutrients such as Mn, Fe, Cu, and Zn; and toxic elements including As, Cr, Ni, and Pb. Wood contains a range of trace elements that play significant roles in processes related to tissue growth [50]. Studies indicate that the mineral content in wood from archaeological sites is significantly higher than that of fresh wood [51]. Besides the elements accumulated during the growth of the tree and its usage, wood also incorporates elements from water and soil where it was preserved. In severely degraded wood tissues, the inorganic content can even exceed 10% of the wood's dry mass [52]. This suggests that as the content of these elements increases, the quality and content of cellulose in archaeological wood decreases. In the Xianyang ancient ferry site samples, the content of S, Ca, Si, Al, Mg, and Na elements exceeded 1%, with S, Ca, and Si contents exceeding 10%—these are recognized examples of elements that accelerate wood degradation (element content in contemporary and archaeological wood) such as copper and its selected compounds [51–54].

X-ray diffraction analysis

As shown in Fig. 7, the XRD spectra were obtained to assess the crystallinity of both fresh *Platycladus orientalis* wood and historical samples collected from the Xianyang Ancient Ferry Site. Cellulose in wood is a biphasic

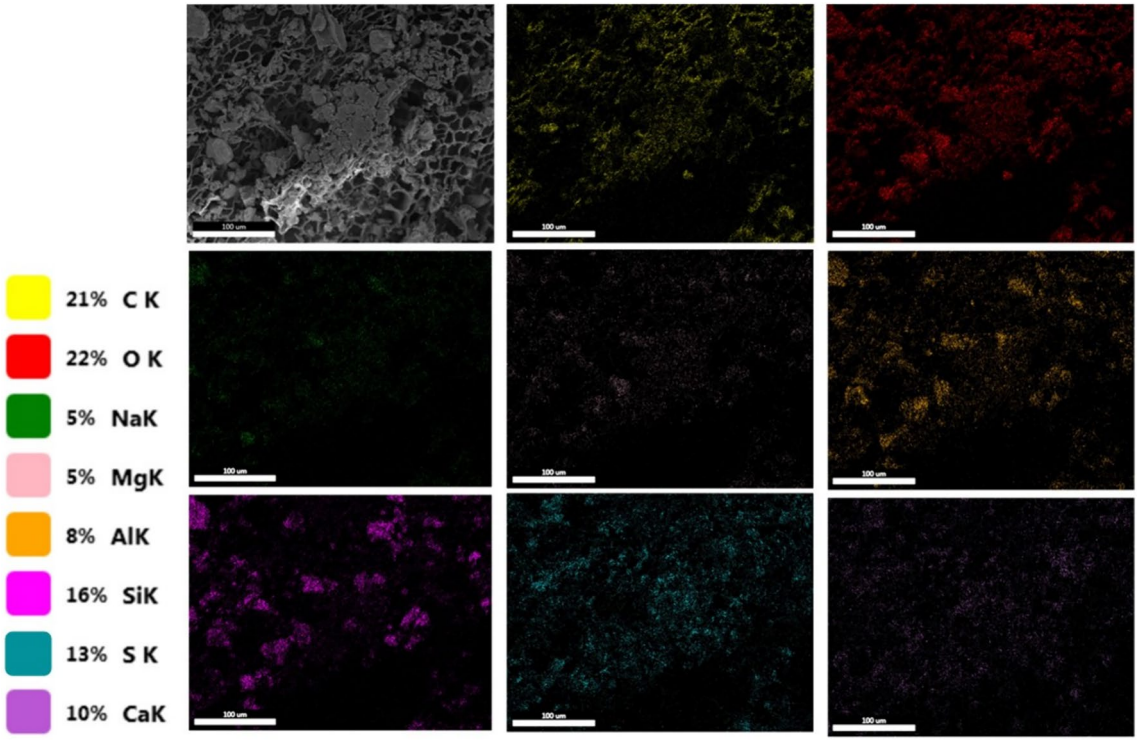

Fig. 6 EDX mapping of the historical wooden sample collected from the Xianyang Ancient Ferry Site

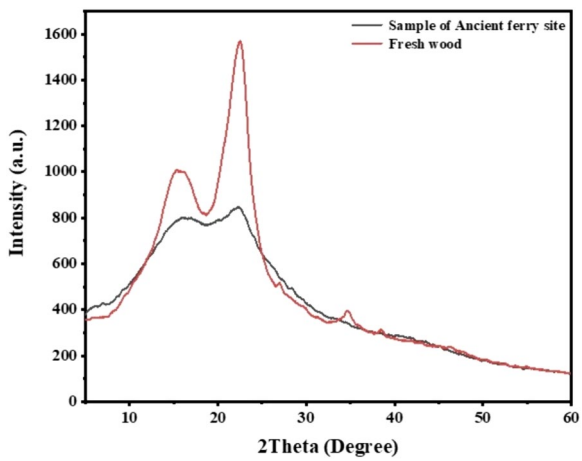

Fig. 7 XRD spectra of historic wooden sample collected from the site and fresh *Platycladus orientalis* wood sample

system composed of crystalline and amorphous regions. In the crystalline regions of cellulose, the molecular chains are oriented and orderly arranged, interconnected laterally through hydrogen bonds formed by hydroxyl groups, thus constituting a crystalline lattice [55]. The crystalline regions of cellulose exhibit better physical properties than those of the amorphous regions, such as tensile strength, density, hardness, and dimensional stability [56, 57]. The diffraction peaks near $2\theta = 22°$ and 34° correspond to the (002) and (040) crystalline plane of wood cellulose respectively, and the peak near $2\theta = 18°$ indicates the amorphous region [58]. As shown in Fig. 7, the diffraction intensity curve of the historical wooden samples is similar to that of the fresh wood, however, the absence of the peak at $2\theta = 34°$ and decreasing intensity of other peaks indicate severe degradation of the wooden components at the site, leading to a decrease in cellulose crystallinity, as supported by the crystallinity calculated using the Segal method [45]. Based on this equation, the relative crystallinity index of fresh *Platycladus orientalis* and the historical wood samples from the Xianyang Ancient Ferry Site is 34.4% and 6.18% respectively. The significant decrease in the relative crystallinity index suggests that the cellulose crystalline index regions in the wooden samples from the site have undergone severe deterioration during long period of underground burial, which further leads to the decrease in mechanical strength and the hydrophobicity of the wooden parts at the site [59].

Infrared spectroscopy analysis

FTIR spectra of the historical wooden samples collected from the site and fresh *Platycladus orientalis* wood are

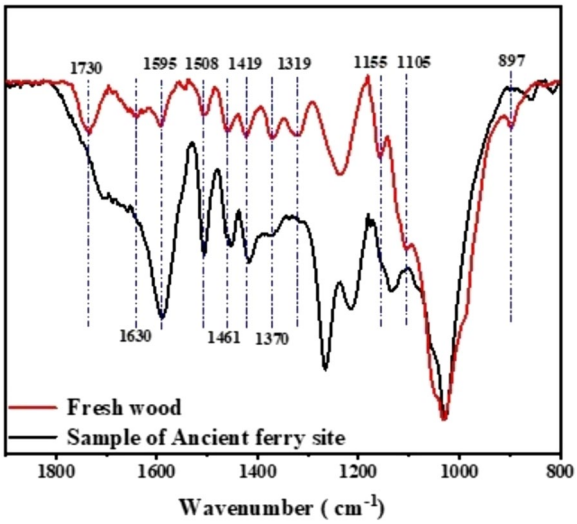

Fig. 8 FTIR spectra of historic wooden samples collected from the site and fresh *Platycladus orientalis* wood samples

shown in Fig. 8. The fresh *Platycladus orientalis* sample has a characteristic absorption peak at 1730 cm^{-1}, which is attributed to the C=O (acetyl) groups in xylan (hemicellulose) [60]. Also, this peak vanished from the FTIR spectrum of the historic wooden sample. The peaks at 1370, 1155, and 1105 cm^{-1} were attributed to C–H deformation stretching vibration, C–O–C stretching vibration, and OH stretching association of cellulose respectively [61]. These peaks, together with the C–H bending vibration of cellulose at 897 cm^{-1}, vanished from the FTIR spectrum of the historical sample. This indicates historic wooden samples had a low concentration of associated hydroxyl groups and significant degradation in the structure of the cellulose crystal zone and hemicellulose.

The absorption peaks at 1595 cm^{-1} and 1508 cm^{-1} are due to the C=C stretching vibrations of the lignin aromatic ring. The peaks at 1461 cm^{-1} and 1419 cm^{-1} correspond to the bending vibrations of CH_2 (C–H) in lignin and carbohydrate, as well as the deformation and expansion vibrations of the benzene ring skeleton combined with C–H in the plane [61–63]. Compared with the fresh *Platycladus orientalis* sample, the peak intensity increases obviously, and some peaks shift to the right. The historic wooden sample peak at 1319 cm^{-1} was significantly decreased, the peak at 1319 cm^{-1} is attributed to the condensation of syringyl ring breathing and condensed guaiacyl in lignin [61]. This suggests that the lignin present in the historic wooden sample from this site has undergone degradation. The observed increase and shift of peaks in the sample may be attributed to a higher degree of degradation of cellulose and hemicellulose compared to lignin, resulting in an increase in relative lignin content upon reduction of cellulose and hemicellulose levels [64].

To quantify the changes in lignin and carbohydrates during the wood degradation process from the ancient ferry site, semi-quantitative calculations were performed following the method proposed by Pandey [60]. The results are shown in Fig. 9. The relative intensities of the lignin band at 1508 cm^{-1} and the carbohydrate bands at 1730, 1370, 1155, and 897 cm^{-1} were calculated using band height ratios. The carbohydrate peaks considered were not severely affected by lignin [60, 65, 66], and include 1730 cm^{-1} for the C=O stretching vibration (acetyl $CH_3C=O$ in hemicellulose), 1370 cm^{-1} for C–H bending vibrations (cellulose and hemicellulose), 1155 cm^{-1} for C–O–C stretching vibrations (cellulose and hemicellulose), and 897 cm^{-1} for C–H bending vibrations (cellulose). When comparing the historic wood samples with the fresh *Platycladus orientalis* sample, an increase in the first four calculated ratios could be interpreted as an indication of significant carbohydrate consumption during burial. Notably, increases in $I_{1508/1730}$ (lignin/hemicellulose), $I_{1508/1155}$ (lignin/cellulose) ratios, and the $I_{1508/897}$ (lignin/cellulose) ratio, suggest that the chemical changes in the historic wood sample predominantly involve cellulose and hemicellulose [52, 67, 68]. For the fresh wood samples, significant changes in the $I_{1508/1730}$, $I_{1508/1155}$, and $I_{1730/897}$ ratios indicate a considerable degree of carbohydrate degradation, particularly the amorphous carbohydrates. The FTIR spectra reveal that the wood components from the ancient ferry site exhibit severe degradation, with substantial degradation of carbohydrates, lignin, hemicellulose, and cellulose.

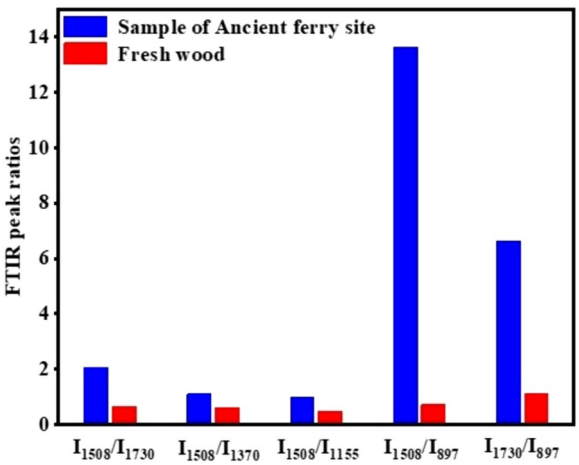

Fig. 9 Histograms showing the values of the ratios calculated between the selected FTIR band heights for historic wooden samples collected from the site and fresh *Platycladus orientalis* wood sample

Thermogravimetric analysis

Thermogravimetric analysis (TGA) is an important method for studying changes in wood composition because the pyrolysis process is essentially the decomposition of various wood components [69]. During TG analysis, each wood sample typically undergoes three distinct stages. The initial phase involves the absorption of heat as the water content is lost within the temperature range of 100–150 ℃, followed by a second phase characterized by an exothermic reaction involving the pyrolytic decomposition of cellulose and hemicellulose within the range of 250–380 ℃. The third phase entails the exothermic process of lignin thermal oxidation within the temperature range of 400–500 ℃. Thermogravimetric spectra of historical wood samples from the Xianyang Ancient Ferry Site and fresh poplar wood are depicted in Fig. 10A, B, respectively.

Figure 10 illustrates the presence of two prominent peaks in both samples, with the second peak attributed to the abundance of hemicellulose and the amorphous portion of cellulose [70, 71]. Hemicellulose decomposes significantly below 350 ℃, while cellulose decomposition occurs primarily between 315 ℃ and 400 ℃, and lignin pyrolysis peak is observed after 400 ℃. Therefore, the peak value at 368 ℃ in the derivative thermogravimetric (DTG) curve of fresh *Platycladus orientalis* (Fig. 10B) is predominantly associated with cellulose decomposition. The second peak value observed in the DTG spectrum of the pile samples from this site shifted towards lower temperatures, accompanied by a decrease in peak intensity and broadening. This phenomenon suggests potential loss of hemicellulose and absence of degradation products [72], while indicating significant degradation of cellulose crystalline regions within the wood and an increased presence of degradation products. The findings from XRD and FTIR analyses align with the hypothesis of poor preservation of wood in the examined samples.

Microbiological analysis

Wood, as a biomass material, is highly susceptible to microbial degradation [73]. The environmental conditions of the archaeological sites can affect the distribution of microorganisms. According to FTIR and XRD analysis, the content of cellulose and hemicellulose in the ancient wood decreased with wood degradation. SEM images show the presence of mold spores within the cell cavities of the ancient wood samples, we therefore isolated and identified microbes from the historical wooden samples collected from the Xianyang Ancient Ferry Site. As shown in Fig. 11, the microbial population of the wooden samples mainly includes *Aspergillus niger, Aspergillus flavus, Penicillium citrinum, Trichoderma,* and *Phanerochaetc chrysoporium*. The SEM results and colony morphology are consistent with Internal Transcribed Spacer (ITS) (Supplementary material) sequencing results. *Phanerochaetc chrysoporium* is one of the well-known microorganisms, type white rot, to effectively accelerate degradation of wooden materials by secreting enzymes to decompose lignin, cellulose, hemicellulose, and pectin [74]. It is able to completely decompose lignin into CO_2 and H_2O, leading to wood deterioration [75, 76], and can also mineralize lignin [77]. With the exclusion of white rot bacteria, the isolated fungal species are not typically categorized as specialized wood degraders; however, many exhibit the capability to degrade wood under suitable environmental circumstances. For instance, it has been established that *Trichoderma* possesses the capability to hydrolyze cellulose [78, 79], and cellulase activity of this species has been screened and shows that it produces the three primary enzymes of the cellulase complex,

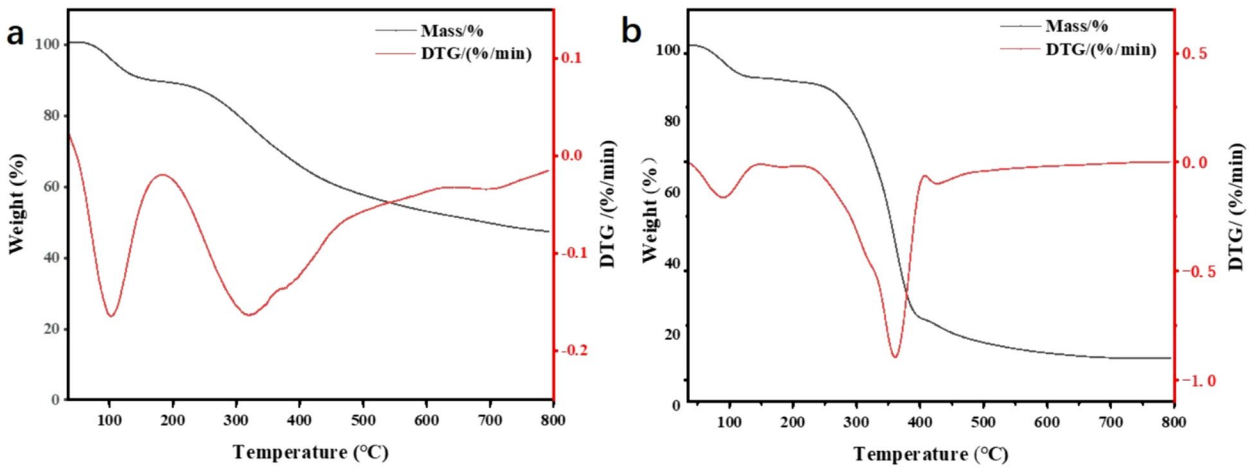

Fig. 10 **A** TG/DTG curves of historic wooden sample collected from the site; **B** TG/DTG curves of fresh *Platycladus orientalis* samples

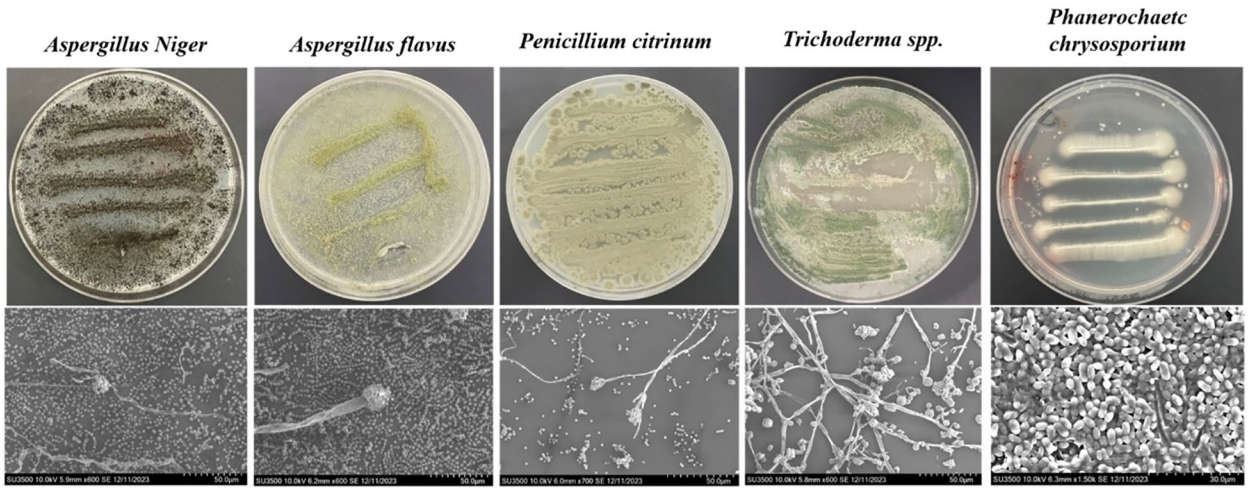

Fig. 11 Colonies, hyphen and spores of microorganisms from the historical wooden samples collected from the Xianyang Ancient Ferry Site

exoglucanase, endoglucanase, and glucosidase [80]. *Aspergillus Niger* and *Aspergillus flavus* are common in soil, especially in an environment with appropriate temperature and humidity.

It is essential for the ecosystem that fungi decompose lignocellulosic materials in terrestrial habitats [81]. As expected, the microorganisms isolated from the Xianyang Ancient Ferry Site included wood-corroding white rot bacteria, while others may be potentially effective decomposers of plant material. The involvement of fungi in the degradation of wooden piles at the Xianyang Ancient Ferry Site is intricately complex. The efficacy of the fungus in deteriorating wood is contingent upon various factors within the controlled environment, for example, encompass synergistic interactions with other fungal enzymes [82], antagonistic relationships with other microorganisms like bacteria [83], and environmental variables such as water content, soil temperature and pH. The wooden pile exhibition area at the Xianyang Ancient Ferry Site is conducive to the growth of certain species, including fungi, due to the absence of temperature and humidity control equipment.

Conclusion

In this study, we systematically evaluated the condition of ancient wooden stakes at the Xianyang Ancient Ferry Site using a series of techniques, arriving at the following conclusions:

1. The wooden stake samples from the Xianyang Ancient Ferry Site are identified as Platycladus orientalists, which are approximately 500 years old, in consistent with historical records about pile-stone construction.
2. SEM–EDX analysis showed that the long-term burial, the cell lumina of the wooden stake samples were filled with spores, and there was a significant increase in the content of inorganic elements, with sulfur (S), calcium (Ca), and silicon (Si) each exceeding 10%. It is hypothesized that these changes were due to long-term burial in moist soil.
3. The wooden stake samples were found to exhibit severe degradation through XRD analysis, TG-DTG analysis, FTIR spectrometry, and the calculation of ratios of intensities for two ranges of absorptions. This degradation was characterized by substantial breakdown of carbohydrates, lignin, hemicellulose, and cellulose, with a particularly significant degradation of cellulose in the crystalline region.
4. The presence of *Aspergillus niger, Aspergillus flavus, Penicillium citrinum, Trichoderma,* and *Phanerochaetc chrysoporium* was identified in the wooden stake samples. Particularly, the *Phanerochaete chrysosporium* contributes to the degradation through the secretion of enzymes that break down lignin, cellulose, hemicellulose, and pectin. The degradation of the stakes is hypothesized to be associated with the activity of *white-rot fungi*.

The unique wood-stone structure of the Xianyang Ancient Ferry Site exemplifies the ingenuity of ancient people and offers insights into modern flood control techniques.This research provides scientific evidence for the selection of reinforcement materials and guides curators and conservators to formulate conservation strategies in the future.

Supplementary Information

The online version contains supplementary material available at https://doi.org/10.1186/s40494-024-01327-w.

Additional file 1.

Acknowledgements
The authors would like to thank the Xianyang Ancient Ferry Site Cultural Relics Administration for their support and cooperation.

Author contributions
The manuscript was prepared through the contributions of all authors. G.T. planned the study together with H.L. and H.X., conducted all data analysis and wrote most of the manuscript. P.F., K.H., H.D., Y.L., and H.L. contributed to the collection of samples in the article. All authors read and approved the final manuscript.

Funding
Special thanks go to Fundamental Research Funds for the Central Universities (GK202304013).

Availability of data and materials
The datasets used and/or analysis results obtained in the current study are available from the corresponding author on request.

Declarations

Competing interests
The authors declare that they have no competing financial interests.

Received: 2 January 2024 Accepted: 14 June 2024
Published online: 24 June 2024

References

1. Bo P. A new ancient ferry site was discovered on the north bank of Weihe River in Xianyang. Shaanxi Daily. 2002.
2. Yafeng W. On water environmental influence from the comprehensive reclamation of WeiHe River at XianYang Section. XianYang: Northwest A&F University; 2006.
3. Lin S, Jijun Z. The multi-sensory landscape experience of "Guanzhong Eight Scenes." Huazhong Archit. 2019;39(9):118–22. https://doi.org/10.13942/j.cnki.hzjz.2019.09.025.
4. Yiming W. Buddhist statues of Sui and Tang dynasties unearthed at Xianyang Ancient Ferry Site. The Silk Road. 2009;22:28–9.
5. Kandilioti G, Makropoulos C. Preliminary flood risk assessment: the case of Athens. Nat Hazards. 2012;61:441–68. https://doi.org/10.1007/s11069-011-9930-5.
6. Heibaum M. Geosynthetics for waterways and flood protection structures–controlling the interaction of water and soil. Geotext Geomembran. 2014;42:374–93. https://doi.org/10.1016/j.geotexmem.2014.06.003.
7. Voronin K, Kabanova M. Chemical-technological research and radiocarbon AMS dating of wall painting fragments from the ruins of the XIIth-XIIIth centuries AD church from archaeological excavations in the city of Smolensk. Russia Heritage Sci. 2020;8:45. https://doi.org/10.1186/s40494-020-00389-w.
8. Shi Y, Zhang J. The flood control heritage of the Yongding River in the late Qing Dynasty surrounding the Marco Polo Bridge section, 1890–189. River Res Appl. 2023;39:1242–54. https://doi.org/10.1002/rra.4017.
9. Lina D, liyan D, Junqi M. Base on the new technique for rescuing the Yellow River, "Dumpling net" is studied and applied to the base. Henan Water conservancy and South-to-North Water Transfer. 2015:121–2.
10. Evette A, Labonne S, Rey F, Liebault F, Jancke O, Girel J. History of bioengineering techniques for erosion control in rivers in Western Europe. Environ Manage. 2009;43:972–84. https://doi.org/10.1007/s00267-009-9275-y.
11. Longhui D. Study on river mark and river camp in Qing Dynasty. Kunming: Yunnan University; 2015.
12. Denan L. On the temporal and spatial evolution of river engineering materials in Ming and Qing Dynasties-Hard materials in Huangyun area as the center. Liaocheng Univ. 2010. https://doi.org/10.16284/j.cnki.cn37-1401/c.2010.01.020.
13. Yibo S. The Functional value of "Yellow River Chant" and thoughts on its inheritance and protection. Literary Theory Crit. 2016. https://doi.org/10.16532/j.cnki.1002-9583.2016.02.025.
14. T M, J B, A C. Los Angeles 196th ACS National Meeting Sept 25–30. Chem Eng News Archive. 1988;66:49–136. https://doi.org/10.1021/cen-v066n031.p049.
15. Guo J, Zhou H, Stevanic JS, Dong M, Yu M, Salmén L, et al. Effects of ageing on the cell wall and its hygroscopicity of wood in ancient timber construction. Wood Sci Technol. 2018;52:131–47. https://doi.org/10.1007/s00226-017-0956-z.
16. Pizzo B, Pecoraro E, Lazzeri S. Dynamic mechanical analysis (DMA) of waterlogged archaeological wood at room temperature. Holzforschung. 2018;72:421–31. https://doi.org/10.1515/hf-2017-0114.
17. Decombeix AL, Boura A, Tomescu AMF. Plant hydraulic architecture through time: lessons and questions on the evolution of vascular systems. IAWA J. 2019;40(3):387–420. https://doi.org/10.1163/22941932-40190254.
18. Walsh-Korb Z, Avérous L. Recent developments in the conservation of materials properties of historical wood. Progress Mater Sci. 2019;102:167–221. https://doi.org/10.1016/j.pmatsci.2018.12.001.
19. Wang D, Dong W, Cao L, Zhu C, Yan J. Deterioration mechanisms of archaeological wood inside the bronze parts of excavated chariots from the Western Han dynasty. J Cult Herit. 2023;62:90–8. https://doi.org/10.1016/j.culher.2023.05.020.
20. Broda M, Popescu C-M. Natural decay of archaeological oak wood versus artificial degradation processes—An FT-IR spectroscopy and X-ray diffraction study. Spectrochim Acta Part A Mol Biomol Spectrosc. 2019;209:280–7. https://doi.org/10.1016/j.saa.2018.10.057.
21. Svedström K, Bjurhager I, Kallonen A, Peura M, Serimaa R. Structure of oak wood from the Swedish warship Vasa revealed by X-ray scattering and microtomography. 2012;66:355-63. https://doi.org/10.1515/hf.2011.157.
22. Broda M, Curling SF, Spear MJ, Hill CAS. Effect of methyltrimethoxysilane impregnation on the cell wall porosity and water vapour sorption of archaeological waterlogged oak. Wood Sci Technol. 2019;53:703–26. https://doi.org/10.1007/s00226-019-01095-y.
23. Bjurhager I, Halonen H, Lindfors EL, Iversen T, Almkvist G, Gamstedt EK, et al. State of degradation in archeological oak from the 17th century Vasa ship: substantial strength loss correlates with reduction in (holo) cellulose molecular weight. Biomacromol. 2012;13(8):2521–7. https://doi.org/10.1021/bm3007456.
24. Łucejko JJ, Mattonai M, Zborowska M, Tamburini D, Cofta G, Cantisani E, et al. Deterioration effects of wet environments and brown rot fungus Coniophora puteana on pine wood in the archaeological site of Biskupin (Poland). Microchem J. 2018;138:132–46. https://doi.org/10.1016/j.microc.2017.12.028.
25. Majka J, Zborowska M, Fejfer M, Waliszewska B, Olek W. Dimensional stability and hygroscopic properties of PEG treated irregularly degraded waterlogged Scots pine wood. J Cult Herit. 2018;31:133–40. https://doi.org/10.1016/j.culher.2017.12.002.
26. Traoré M, Kaal J, Martínez CA. Potential of pyrolysis-GC–MS molecular fingerprint as a proxy of modern age Iberian shipwreck wood preservation. J Anal Appl Pyrol. 2017;126:1–13. https://doi.org/10.1016/j.jaap.2017.07.003.
27. Oron A, Liphschitz N, Held BW, Galili E, Klein M, Linker R, et al. Characterization of archaeological waterlogged wooden objects exposed on the hyper-saline Dead Sea shore. J Archaeol Sci Rep. 2016;9:73–86. https://doi.org/10.1016/j.jasrep.2016.06.049.
28. Łucejko JJ, Modugno F, Ribechini E, Tamburini D, Colombini MP. Analytical instrumental techniques to study archaeological wood degradation. Appl Spectrosc Rev. 2015;50:584–625. https://doi.org/10.1080/05704928.2015.1046181.
29. Pedersen NB, Gierlinger N, Thygesen LG. Bacterial and abiotic decay in waterlogged archaeological *Picea abies* (L.) Karst studied by confocal Raman imaging and ATR-FTIR spectroscopy. Holzforschung. 2015;69:103–12. https://doi.org/10.1515/hf-2014-0024.

30. Xia Y, Chen T, Wen J-l, Zhao Y-L, Qiu J, Sun R. Multi-analysis of chemical transformations of lignin macromolecules from waterlogged archaeological wood. Int J Bio Macromol. 2018;109:407–16. https://doi.org/10.1016/j.ijbiomac.2017.12.114.
31. P L. The study of crystal structure and thermal decomposition of Paphia undulate using XRD, TGA and FTIR techniques. Annals New York Acad Sci. 1958;76(76):838–49.
32. Blanchette RA. Deterioration in historic and archaeological woods from terrestrial sites. Art Bio Conser. 2003;16:328–47.
33. Timar LG, Cionca M, Porojan M. Wood species for the biedermeier furniture–a microscopic characterisation for scientific conservation. Int J Conser Sci. 2010;1:3–12.
34. Baas P, Wheeler EA. Wood Identification–a review. Iawa. Journal. 1998;19:241–64. https://doi.org/10.1163/22941932-90001528.
35. Giachi G, Guidotti MC, Lazzeri S, Sozzi L, Macchioni N. Wood identification of the headrests from the collection of the Egyptian Museum in Florence. J Archaeol Sci Rep. 2016;9:340–6. https://doi.org/10.1016/j.jasrep.2016.08.027.
36. Schwarze FW. Wood decay under the microscope. Fungal Bio Rev. 2007;21:133–70. https://doi.org/10.1016/j.fbr.2007.09.001.
37. Cartwright CR. The principles, procedures and pitfalls in identifying archaeological and historical wood samples. Ann Bot. 2015;116:1–13. https://doi.org/10.1093/aob/mcv056.
38. Richter HG, Dallwitz M. Commercial timbers: descriptions, illustrations, identification, and information retrieval, Delta. 2000. https://www.delta-intkey.com/wood/en/index.htm.
39. Bernabei M, Macchioni N, Pizzo B, Sozzi L, Lazzeri S, Fiorentino L, et al. The wooden foundations of Rialto Bridge (Ponte di Rialto) in Venice: technological characterisation and dating. J Cult Herit. 2019;36:85–93. https://doi.org/10.1016/j.culher.2018.07.015.
40. Blanchette RA. A review of microbial deterioration found in archaeological wood from different environments. Int Biodeteriorat Biodegradat. 2000;46:189–204. https://doi.org/10.1016/S0964-8305(00)00077-9.
41. Cartwright CR. Identifying ancient Egyptian coffin woods from the Fitzwilliam Museum, Cambridge using scanning electron microscopy. Ancient Egyptian Coffins. 2018;8:39.
42. Cartwright CR. Understanding wood choices for ancient panel painting and mummy portraits in the APPEAR project through scanning electron microscopy. In M. Svoboda & C. R. Cartwright (Eds.), Mummy portraits of Roman Egypt: Emerging research from the APPEAR project (pp. 16–23). J. Paul Getty Museum, Los Angeles Getty Publications. 2020.
43. Hormes A, Blaauw M, Dahl SO, Nesje A, Possnert G. Radiocarbon wiggle-match dating of proglacial lake sediments–implications for the 82ka event. Quarter Geochronol. 2009;4:267–77. https://doi.org/10.1016/j.quageo.2008.12.004.
44. Martínez-Sevilla F, Herrero-Otal M, Martín-Seijo M, Santana J, Lozano Rodríguez JA, Maicas Ramos R, et al. The earliest basketry in southern Europe: hunter-gatherer and farmer plant-based technology in Cueva de los Murciélagos (Albuñol). Sci Adv. 2023. https://doi.org/10.1126/sciadv.adi3055.
45. Segal L, Creely JJ, Martin AE, Conrad CM. An empirical method for estimating the degree of crystallinity of native cellulose using the X-ray diffractometer. Text Res J. 1959;29:786–94. https://doi.org/10.1177/004051755902901003.
46. Jun P, Cai Z, Wei C. Unearthed woods from no.1 Qingong Mausoleum at fengxiang Shaanxi. J Northwest Forest Univer. 1990;3:10–6.
47. Laskowska A, Majewska K, Kozakiewicz P, Mamiński M, Bryk G. Case study of anatomy, physical and mechanical properties of the sapwood and heartwood of random tree *Platycladus orientalis* (L.) Franco from South-Eastern Poland. Forests. 2021;12:925. https://doi.org/10.3390/f12070925.
48. Macchioni N, Capretti C, Sozzi L, Pizzo B. Grading the decay of waterlogged archaeological wood according to anatomical characterisation The case of the Fiavé site (N-E Italy). Int Biodeteriorat Biodegradat. 2013;84:54–64. https://doi.org/10.1016/j.ibiod.2013.05.028.
49. Zając G, Szyszlak-Bargłowicz J, Gołębiowski W, Szczepanik M. Chemical characteristics of biomass ashes. Energies. 2018;11(11):2885.
50. Fromm J. Wood formation of trees in relation to potassium and calcium nutrition. Tree Physiol. 2010;30:1140–7. https://doi.org/10.1093/treephys/tpq024.
51. High KE, Penkman KEH. A review of analytical methods for assessing preservation in waterlogged archaeological wood and their application in practice. Heritage Sci. 2020;8:83. https://doi.org/10.1186/s40494-020-00422-y.
52. Hedges JI. The Chemistry of Archaeological Wood. Archaeological Wood. Advances in Chemistry. 225: American Chemical Society; 1989. p. 111–40.
53. Henry WP. Non-Enzymatic Iron, Manganese, and Copper Chemistry of Potential Importance in Wood Decay. Wood Deterioration and Preservation. ACS Symposium Series. 845: American Chemical Society; 2003. p. 175–95.
54. Zhu X, Wang X, Ok YS. The application of machine learning methods for prediction of metal sorption onto biochars. J Hazard Mater. 2019;378:120727. https://doi.org/10.1016/j.jhazmat.2019.06.004.
55. Mai B, Liu N, Liu J, Liu D, Li J, Wang J, et al. Analysis and appraisal of fascine in Shahe ancient bridge ruins, Xi'an, Shaanxi. China Heritage Sci. 2022;10:24. https://doi.org/10.1186/s40494-022-00659-9.
56. Isogai A. Development of completely dispersed cellulose nanofibers. Proc Jpn Acad Ser B Phys Biol Sci. 2018;94:161–79. https://doi.org/10.2183/pjab.94.012.
57. Eichhorn SJ, Dufresne A, Aranguren M, Marcovich NE, Capadona JR, Rowan SJ, et al. Review: current international research into cellulose nanofibres and nanocomposites. J Mater Sci. 2010;45:1–33. https://doi.org/10.1007/s10853-009-3874-0.
58. Park S, Baker JO, Himmel ME, Parilla PA, Johnson DK. Cellulose crystallinity index: measurement techniques and their impact on interpreting cellulase performance. Biotechnol Biofuels. 2010;3:10. https://doi.org/10.1186/1754-6834-3-10.
59. Ling S, Kaplan DL, Buehler MJ. Nanofibrils in nature and materials engineering. Nat Rev Mater. 2018;3:18016. https://doi.org/10.1038/natrevmats.2018.16.
60. Pandey KK, Pitman AJ. FTIR studies of the changes in wood chemistry following decay by brown-rot and white-rot fungi. Int Biodeterior Biodegradation. 2003;52:151–60. https://doi.org/10.1016/S0964-8305(03)00052-0.
61. Popescu C-M, Popescu M-C, Vasile C. Characterization of fungal degraded lime wood by FT-IR and 2D IR correlation spectroscopy. Microchem J. 2010;95:377–87. https://doi.org/10.1016/j.microc.2010.02.021.
62. Popescu M-C, Popescu C-M, Lisa G, Sakata Y. Evaluation of morphological and chemical aspects of different wood species by spectroscopy and thermal methods. J Mol Struct. 2011;988:65–72. https://doi.org/10.1016/j.molstruc.2010.12.004.
63. Nguyen H, Lagarde F, Louarn G, Daniel P. A new way to discriminate polluted wood by vibrational spectroscopies. Talanta. 2017;167:436–41. https://doi.org/10.1016/j.talanta.2017.02.032.
64. Özgenç Ö, Durmaz S, Boyaci IH, Eksi-Kocak H. Determination of chemical changes in heat-treated wood using ATR-FTIR and FT Raman spectrometry. Spectrochim Acta Part A Mol Biomol Spectrosc. 2017;171:395–400. https://doi.org/10.1016/j.saa.2016.08.026.
65. Faix O. Classification of lignins from different botanical origins by FT-IR spectroscopy. Am Chem Soc. 1991;45(21):28. https://doi.org/10.1515/hfsg.1991.45.s1.21.
66. Schwanninger M, Rodrigues JC, Pereira H, Hinterstoisser B. Effects of short-time vibratory ball milling on the shape of FT-IR spectra of wood and cellulose. Vib Spect. 2004;36:23–40. https://doi.org/10.1016/j.vibspec.2004.02.003.
67. Hedges JI, Cowie GL, Ertel JR, James Barbour R, Hatcher PG. Degradation of carbohydrates and lignins in buried woods. Geochim Cosmochim Acta. 1985;49:701–11. https://doi.org/10.1016/0016-7037(85)90165-6.
68. Rowell RM, Barbour RJ. Archaeological wood: properties, chemistry, and preservation. ChemInform. 1990; 21.
69. Chen M, Ma Y, Zhang B, Hu Y. Feasibility study on conservation of water-saturated archaeological wood in earthen sites by hot air with different humidity. Eur Phy J Plus. 2024;139:55. https://doi.org/10.1140/epjp/s13360-024-04882-0.
70. González-Díaz E, Alonso-López J-M. Characterization by thermogravimetric analysis of the wood used in Canary architectural heritage. J Cult Herit. 2017;23:111–8. https://doi.org/10.1016/j.culher.2016.09.002.
71. Zoia L, Salanti A, Orlandi M. Chemical characterization of archaeological wood: softwood vasa and hardwood Riksapplet case studies. J Cult Herit. 2015;16:428–37. https://doi.org/10.1016/j.culher.2014.09.015.
72. Romagnoli M, Galotta G, Antonelli F, Sidoti G. Micro-morphological, physical and thermogravimetric analyses of waterlogged archaeological wood

from the prehistoric village of Gran Carro (Lake Bolsena-Italy). J Cult Herit. 2018;33:30–8. https://doi.org/10.1016/j.culher.2018.03.012.
73. Abdel-Azeem AM, Held BW, Richards JE, Davis SL, Blanchette RA. Assessment of biodegradation in ancient archaeological wood from the Middle Cemetery at Abydos Egypt. PLoS ONE. 2019. https://doi.org/10.1371/journal.pone.0213753.
74. Baramee S, Phitsuwan P, Waeonukul R, Pason P, Tachaapaikoon C, Kosugi A, et al. Alkaline xylanolytic–cellulolytic multienzyme complex from the novel anaerobic alkalithermophilic bacterium Cellulosibacter alkalithermophilus and its hydrolysis of insoluble polysaccharides under neutral and alkaline conditions. Process Biochem. 2015;50:643–50. https://doi.org/10.1016/j.procbio.2015.01.019.
75. Kirk TK, Farrell RL. Enzymatic "combustion": the microbial degradation of lignin. Annu Rev Microbiol. 1987;41:465–505. https://doi.org/10.1146/annurev.mi.41.100187.002341.
76. Li F, Zhang P, Zhang G, Tang X, Wang S, Jin S. Enhancement of corn stover hydrolysis with rumen fluid pretreatment at different solid contents: effect, structural changes and enzymes participation. Int Biodeterior Biodegradation. 2017;119:405–12. https://doi.org/10.1016/j.ibiod.2016.10.038.
77. Lundell TK, Mäkelä MR, Hildén K. Lignin-modifying enzymes in filamentous basidiomycetes–ecological, functional and phylogenetic review. J Basic Microbiol. 2010;50:5–20. https://doi.org/10.1002/jobm.200900338.
78. Puls J, Wood TM. The degradation pattern of cellulose by extracellular cellulases of aerobic and anaerobic microorganisms. Biores Technol. 1991;36:15–9. https://doi.org/10.1016/0960-8524(91)90096-3.
79. Pournou A, Bogomolova E. Fungal colonization on excavated prehistoric wood: implications for in-situ display. Int Biodeterior Biodegradation. 2009;63:371–8. https://doi.org/10.1016/j.ibiod.2008.11.001.
80. Yeoh HH, Tan TK, Tian KE. Cellulolytic enzymes of fungi isolated from wood materials. Mycopathologia. 1984;87:51–5. https://doi.org/10.1007/BF00436628.
81. Berg B, Laskowski R. Decomposers: soil microorganisms and animals. Advances in ecological research. 38: Academic Press; 2005. p. 73–100.
82. Setälä H, McLean MA. Decomposition rate of organic substrates in relation to the species diversity of soil saprophytic fungi. Oecologia. 2004;139:98–107. https://doi.org/10.1007/s00442-003-1478-y.
83. Romani AM, Fischer H, Mille-Lindblom C, Tranvik LJ. Interactions of bacteria and fungi on decomposing litter: differential extracellular enzyme activities. Ecology. 2006;87:2559–69. https://doi.org/10.1890/0012-9658(2006)87[2559:IOBAFO]2.0.CO;2.

Publisher's Note